

1    **Extreme N<sub>2</sub>O accumulation in the coastal oxygen minimum zone off Peru**

2    Annette Kock<sup>1</sup>, Damian L. Arévalo-Martínez<sup>1</sup>, Carolin R. Löscher<sup>2</sup>, Hermann W. Bange<sup>1</sup>

3    <sup>1</sup>GEOMAR Helmholtz Centre for Ocean Research Kiel, Düsternbrooker Weg 20, 24105 Kiel, Germany

4    <sup>2</sup>Institute of General Microbiology, Christian-Albrechts University Kiel, Am Botanischen Garten 1-9, 24118 Kiel, Germany

5    Correspondence to: Annette Kock, [akock@geomar.de](mailto:akock@geomar.de)

6

7

8

## 9     **Abstract**

10     Depth profiles of nitrous oxide ( $\text{N}_2\text{O}$ ) were measured during six cruises to the upwelling area and  
11     oxygen minimum zone (OMZ) off Peru in 2009 and 2012/2013, covering both the coastal shelf region  
12     and the adjacent open ocean.  $\text{N}_2\text{O}$  profiles displayed a strong sensitivity towards oxygen  
13     concentrations. Open ocean profiles with distances to the shelf break larger than the first baroclinic  
14     Rossby radius of deformation showed a transition from a broad maximum close to the equator to a  
15     double-peak structure south of  $5^\circ\text{S}$  where the oxygen minimum was more pronounced. Maximum  
16      $\text{N}_2\text{O}$  concentrations in the open ocean were about 80 nM. A linear relationship between  $\Delta\text{N}_2\text{O}$  and  
17     apparent oxygen utilization (AOU) could be found for all measurements within the upper oxycline,  
18     with a slope similar to studies in other oceanic regions. In contrast,  $\text{N}_2\text{O}$  profiles close to the shelf  
19     revealed a much higher variability, and  $\text{N}_2\text{O}$  concentrations higher than 100 nM were often observed.  
20     The highest  $\text{N}_2\text{O}$  concentration measured at the shelf was  $\sim 850$  nM. Due to the extremely sharp  
21     oxygen gradients at the shelf,  $\text{N}_2\text{O}$  maxima occurred in very shallow water depths of less than 50 m.  
22     In the coastal area, a linear relationship between  $\Delta\text{N}_2\text{O}$  and AOU could not be observed as extremely  
23     high  $\Delta\text{N}_2\text{O}$  values were scattered over the full range of oxygen concentrations. The data points that  
24     showed the strongest deviation from a linear  $\Delta\text{N}_2\text{O}$ /AOU relationship also showed signals of intense  
25     nitrogen loss. These results indicate that the coastal upwelling at the Peruvian coast and the  
26     subsequent strong remineralization in the water column causes conditions that lead to extreme  $\text{N}_2\text{O}$   
27     accumulation, most likely due to the interplay of intense mixing and high rates of remineralization  
28     which lead to a rapid switching of the OMZ waters between anoxic and oxic conditions. This, in turn,  
29     could trigger incomplete denitrification or pulses of increased nitrification with extreme  $\text{N}_2\text{O}$   
30     production.

31

32

## 1 Introduction

Nitrous oxide ( $\text{N}_2\text{O}$ ) acts as a strong atmospheric greenhouse gas and contributes substantially to the stratospheric ozone depletion (IPCC, 2013; WMO, 2011). The ocean is a major source for  $\text{N}_2\text{O}$  as it is naturally produced in the water column (Ciais et al., 2013; Bange, 2008). While in large parts of the surface ocean  $\text{N}_2\text{O}$  concentrations are close to saturation, high emissions of  $\text{N}_2\text{O}$  have been observed in upwelling areas where subsurface waters enriched in  $\text{N}_2\text{O}$  are transported to the surface (e.g. Nevison et al., 2004). The global distribution of  $\text{N}_2\text{O}$  in the ocean is closely linked to the oceanic oxygen distribution, and particularly high supersaturations are found in upwelling areas which overlay pronounced oxygen minimum zones (OMZ), e.g. in the Arabian Sea (Bange et al., 2001) or in the eastern South Pacific Ocean (Charpentier et al., 2010).

These OMZs are key regions for marine nitrogen (N) cycling where active N loss via canonical denitrification and anaerobic ammonium oxidation (anammox) takes place. Particularly in areas where the OMZ is fuelled by high export production, high rates of denitrification and anammox, but also other N transformation processes, such as nitrification, have been observed (Hu et al., 2015; Kalvelage et al., 2013). Oceanic  $\text{N}_2\text{O}$  is mainly produced by nitrification and denitrification, and the interplay of these processes governs the  $\text{N}_2\text{O}$  distribution in OMZs (Bange, 2008).

The relationship between  $\text{N}_2\text{O}$  and oxygen concentrations in the ocean is often described by comparing excess  $\text{N}_2\text{O}$  ( $\Delta\text{N}_2\text{O}$ ) and the apparent oxygen utilization (AOU). As nitrification is one major process accompanying the remineralization of organic matter, a positive correlation between the excess  $\text{N}_2\text{O}$  ( $\Delta\text{N}_2\text{O}$ ) and the apparent oxygen utilization (AOU) is often interpreted as an indication for nitrification as the main  $\text{N}_2\text{O}$  production pathway (e.g. Walter et al., 2006; Forster et al., 2009).

Nitrification can either be performed by bacteria (Arp and Stein, 2003) or archaea (Walker et al., 2010). Recent studies indicate that archaea may dominate marine  $\text{N}_2\text{O}$  production under oxic conditions (Löscher et al., 2012; Santoro et al., 2011). The production mechanisms and

environmental controls of archaeal  $\text{N}_2\text{O}$  production are subject to ongoing research, however (Stieglmeier et al., 2014).

An increase in the  $\Delta\text{N}_2\text{O}/\text{AOU}$  ratio at low oxygen concentrations has been observed in several studies in different oceanic areas with reduced oxygen concentrations (Ryabenko et al., 2012; Upstill-Goddard et al., 1999; De Wilde and Helder, 1997). This could be explained by several processes: During nitrification,  $\text{N}_2\text{O}$  can either be produced as a side product from the oxidation of ammonium to nitrite, or from the reduction of nitrite to  $\text{N}_2\text{O}$ , a process known as nitrifier-denitrification (Stein, 2011). Nitrifier-denitrification has been identified as an important production pathway of  $\text{N}_2\text{O}$  at low oxygen concentrations and may thus be responsible for the increased  $\text{N}_2\text{O}$  production under these conditions (Ni et al., 2014). An increase in the  $\text{N}_2\text{O}$  yield of nitrification has indeed been observed in laboratory experiments with bacterial (Goreau et al., 1980) and archaeal ammonium oxidizers (Löscher et al., 2012). The extent to which ammonium oxidation or the nitrifier-denitrification pathway are responsible for  $\text{N}_2\text{O}$  production is yet not well determined (Ostrom et al., 2000; Ni et al., 2014), particularly for archaeal nitrification (Löscher et al., 2012; Santoro et al., 2011; Stieglmeier et al., 2014).

Additional  $\text{N}_2\text{O}$  production from denitrification has also been proposed as a potential mechanism leading to an increased  $\Delta\text{N}_2\text{O}/\text{AOU}$  at low oxygen concentrations (e.g. Farías et al., 2009; Ji et al., 2015). During denitrification, the canonical reduction of nitrate to molecular nitrogen,  $\text{N}_2\text{O}$  evolves as an intermediate product. Denitrification is stimulated by the supply of organic carbon or hydrogen sulfide (Chang et al., 2014; Dalsgaard et al., 2014; Galan et al., 2014), and active denitrification is restricted to suboxic to anoxic conditions (e.g. Firestone et al., 1980; Dalsgaard et al., 2014). Depending on the environmental conditions,  $\text{N}_2\text{O}$  production or consumption due to denitrification can be observed in the environment. There has been evidence that  $\text{N}_2\text{O}$  consumption is more sensitive to trace amounts of oxygen than  $\text{N}_2\text{O}$  production. This could lead to  $\text{N}_2\text{O}$  accumulation when oxygen is present in low concentrations (Tiedje, 1988). Exceptionally high  $\text{N}_2\text{O}$  concentrations off the West Indian Coast were thus associated with an increased  $\text{N}_2\text{O}$  production

from denitrification during transient oxygen concentrations (Naqvi et al., 2000). In a recent study it was furthermore shown that  $\text{N}_2\text{O}$  production from denitrification could be stimulated by  $\text{H}_2\text{S}$  addition (Dalsgaard et al., 2014) which could indicate a coupling between  $\text{N}_2\text{O}$  production and sulfur cycling.

At oxygen concentrations below a threshold value of 4 - 10  $\mu\text{M}$ , (Nevison et al., 2003; Ryabenko et al., 2012; Cornejo and Farias, 2012), consumption of  $\text{N}_2\text{O}$  in the water column is observed, which leads to a breakdown in the previously described positive  $\Delta\text{N}_2\text{O}/\text{AOU}$  relationship. The exact oxygen concentration at which  $\text{N}_2\text{O}$  consumption starts is not yet well determined, however (Cornejo and Farias, 2012; Zamora et al., 2012).  $\text{N}_2\text{O}$  consumption has been associated with denitrification as the only known process to consume  $\text{N}_2\text{O}$  in OMZ waters (Cornejo and Farias, 2012). Although rate measurements only rarely detected active denitrification in the water column of the ETSP (Kalvelage et al., 2013; Hamersley et al., 2007; Thamdrup et al., 2006), the widespread  $\text{N}_2\text{O}$  consumption in the OMZ core is an indicator for active denitrification (Farias et al., 2007).

There is a strong indication that at low oxygen concentrations nitrification and denitrification may take place in close proximity (Kalvelage et al., 2011), and the  $\text{N}_2\text{O}$  production and consumption under these conditions are strongly influenced by the interaction of both processes (Ji et al., 2015).

Measurements of  $\text{N}_2\text{O}$  consumption rates in the eastern tropical North Pacific Ocean (ETNP) furthermore provided evidence for a rapid  $\text{N}_2\text{O}$  cycling, although depth profiles of  $\text{N}_2\text{O}$  seemed to be relatively invariant over time (Babbin et al., 2015). These quasi-stable conditions may be disturbed by rapid changes in the environmental conditions.

The eastern tropical South Pacific Ocean (ETSP) harbors one of the four major eastern boundary upwelling systems (EBUS): alongshore trade winds induce offshore Ekman transport of the surface water masses which leads to strong coastal upwelling off Peru and Chile (Chavez and Messié, 2009).

While year-round upwelling and high primary productivity can be observed along the Peruvian coast (Messie et al., 2009), the highest upwelling intensity can be observed during austral winter, whereas primary production seems to be higher during autumn and spring (Pennington et al., 2006), which

108 may be caused by nutrient and light limitation during phases of intense upwelling (Echevin et al.,  
109 2008).

110 The region is influenced by strong seasonal and interannual variability caused by the influence of  
111 Equatorial Kelvin waves and the El Niño Southern Oscillation (ENSO). ENSO could cause the  
112 interruption of the upwelling during El Niño events (Dewitte et al., 2012; Graco et al., 2016). While  
113 the OMZ core is largely unaffected by ENSO, a deepening of the upper oxycline and the re-  
114 oxygenation of the Peruvian shelf due to the propagation of coastal trapped waves can be observed  
115 (Gutierrez et al., 2008).

116 The ETSP is characterized by one of the largest and most intense OMZs in the oceans, extending from  
117 the Peruvian shelf about 1000 km offshore with a maximum thickness of more than 600 m  
118 (Fuenzalida et al., 2009). It is located in the shadow zone of large ocean current systems which leads  
119 to a sluggish ventilation and long residence times of waters within the OMZ (Karstensen et al., 2008).  
120 Equatorial current bands such as the Equatorial Undercurrent (EUC) and the Southern Subsurface  
121 Countercurrents (SSCC) supply waters to the ETSP which leads to slightly elevated oxygen  
122 concentrations in the northern part of our study area, with minimum oxygen concentrations of 10 -  
123 20  $\mu\text{M}$  (Stramma et al., 2010), whereas oxygen concentrations below 3  $\mu\text{M}$  are common in the OMZ  
124 core south of 5°S (Paulmier et al., 2006). The equatorial current bands also feed the poleward Peru-  
125 Chile Undercurrent (PCUC) which is the main source for waters upwelled along the coast (Montes et  
126 al., 2010; Chaigneau et al., 2013) and which transports Equatorial Subsurface Water (ESSW)  
127 southward. During its spreading, the ESSW is subject to oxygen depletion and mixing with  
128 surrounding water masses, e.g. the Antarctic Intermediate Water (AAIW) below and the Eastern  
129 South Pacific Intermediate Water (ESPIW) which originates from the South (Wyrski, 1967; Chaigneau  
130 et al., 2013). Mixing of different water masses in the upwelling zone creates a distinct coastal water  
131 mass which is called Cold Coastal Water (CCW) (Pietri et al., 2013).

High primary production and high remineralization rates in the underlying waters lead to a further drawdown in subsurface oxygen concentrations to near-depleted conditions (Karstensen et al., 2008). Active N loss is observed in large parts of the OMZ which is reflected in a pronounced secondary nitrite maximum and a strong nitrogen deficit in the OMZ core (Codispoti et al., 1986). The OMZ furthermore frequently extends over large parts of the Peruvian shelf where sulfidic conditions within the water column can be observed (Schunck et al., 2013).

Here we present N<sub>2</sub>O measurements in the water column off Peru from six measurement campaigns in the ETSP. Previous depth profile measurements in this area showed a pronounced double-peak structure off South Peru which merged into a broad maximum north of 5°N (Cornejo and Farias, 2012; Ryabenko et al., 2012). Surface N<sub>2</sub>O measurements off Peru furthermore revealed extraordinarily high emissions from the Peruvian shelf area which corresponded to extremely high surface and subsurface N<sub>2</sub>O concentrations (Arévalo-Martínez et al., 2015).

144

145

146

## 2 Methods

In total, 146 depth profiles (0~4200 m) of N<sub>2</sub>O were measured on two cruises between December 2008 and February 2009 (M77-3 & M77-4) and four cruises between October 2012 and March 2013 (M90 - M93) to the upwelling area and the adjacent open ocean off Peru onboard the German research vessel Meteor. The Southern Oscillation Indices (<http://www.ncdc.noaa.gov/teleconnections/enso/indicators/soi/>) from 2008/2009 and 2012/2013 did not indicate the presence of an El Niño event during our measurement campaigns and similar conditions between both measurement campaigns could be expected. The locations of the sampled stations are shown in Fig. 1. While the M77-4 and M90 cruises mainly covered the open ocean area, the M77-3 and M91-M93 cruises mainly took place in the Peruvian shelf area. The work was part of the German DFG collaborative research project (SFB) 754 (<https://www.sfb754.de/>) and the BMBF project SOPRAN (Surface Ocean PRocesses in the ANthropocene, [www.sopran.pangaea.de](http://www.sopran.pangaea.de)). The N<sub>2</sub>O data set described here has been archived in MEMENTO, the MarinE MethanE and NiTrous Oxide database (<https://memento.geomar.de>) (Kock and Bange, 2015).

Triplicate samples were taken from 10 L Niskin bottles mounted on a rosette water sampler or a pump-CTD (M77-3) in 25 ± 0.11 mL (M77-3 & M77-4) and 20 ± 0.14 mL (M90 - M93) opaque glass vials and sealed with butyl rubber stoppers and aluminum caps, thereby avoiding the inclusion of air bubbles.

Samples were treated with 0.2 mL (M77-3 & M77-4) and 0.05 mL (M90 - M93) of a saturated mercuric chloride solution directly after the sampling to inhibit microbial N<sub>2</sub>O production or consumption. The samples were either analyzed onboard (M77-3 & M77-4, M91, partly M90 & M93) within a few days or shipped to GEOMAR by air freight for later analysis (M92, partly M90 & M93). Samples that were shipped to Germany were additionally sealed with paraffin wax and stored upside down to avoid the formation of air bubbles in the samples due to temperature and pressure changes during transportation.



Samples were analyzed using a static equilibration method: 10 mL helium (99.9999%, AirLiquide, Düsseldorf, Germany) was manually injected into each vial which was equipped with a second syringe to collect the overflowing water. Vials with added headspace were vigorously shaken for about 20 s and allowed to equilibrate at ambient temperature for a minimum of two hours. A subsample of the equilibrated headspace was manually injected into a GC-ECD system (Hewlett-Packard 5890 Series II, Agilent Technologies, Santa Clara, CA, USA), equipped with a 6' 1/8" packed column (molsieve, 5Å, W. R. Grace & Co.-Conn., Columbia, MY). The GC was operated at 190 °C, using argon/methane (95%/5%, ECD purity, AirLiquide, Düsseldorf, Germany) as carrier gas at a flow rate of 30 mL min<sup>-1</sup>.

The GC was calibrated on a daily basis with a minimum of 2 (M77-3 & M77-4) or 4 (M90 - M93) different standard gas mixtures (N<sub>2</sub>O in synthetic air, Deuste-Steininger GmbH, Mühlhausen, Germany and Westfalen AG, Münster, Germany). Standard gases were either injected as pure gas or further diluted with helium (1:3, 1:1 or 3:1) to obtain additional standard gas concentrations. Our standard gases were calibrated against NOAA primary standards at the Max Planck Institute for Biogeochemistry in Jena, Germany, if the standard gas concentrations were within the calibration range of the NOAA gases. Gases with N<sub>2</sub>O concentrations outside the NOAA calibration range were internally calibrated using an LGR N<sub>2</sub>O/CO analyzer (Los Gatos Research, Mountain View, CA, USA), which was proven to have a linear response and minimal drift within the calibration range (Arévalo-Martínez et al., 2013). The N<sub>2</sub>O concentration in the samples was calculated according to Walter et al. (2006) using the solubility function of Weiss and Price (1980). The average precision of the measurements, calculated as median standard deviation from triplicate measurements, was 0.7 nM.

$\Delta N_2O$  was calculated as the difference between the in-situ concentration  $[N_2O]_w$  and the equilibrium concentration  $[N_2O]_{eq}$ :

$$\Delta N_2O = [N_2O]_w - [N_2O]_{eq} \quad (1)$$

197 We used the contemporary atmospheric mixing ratio measured at Cape Grim, Tasmania  
198 (<http://agage.mit.edu/data/agage-data>) for the calculation of  $[N_2O]_{eq}$ . This calculation  
199 underestimates the  $N_2O$  excess in subsurface waters which have been isolated from the surface for a  
200 long time as it does not account for the increase in the atmospheric mixing ratio since the beginning  
201 of the industrial revolution (Freing et al., 2009). The use of the contemporary  $N_2O$  mixing ratio of  
202 2013 would lead to a maximum ~17% overestimate of  $[N_2O]_{eq}$ , thus leading to only a small error  
203 compared to the maximum  $N_2O$  concentrations measured in our study, and the use of the  
204 contemporary atmospheric mixing ratio still allows a qualitative analysis of the  $\Delta N_2O/AOU$   
205 relationship in order to investigate the formation and consumption processes of  $N_2O$ .

206 The potential temperature of the water parcel at a certain depth was calculated using the Gibbs  
207 Seawater Oceanographic Toolbox (McDougall and Barker, 2011).

208 Oxygen concentrations were measured either with a Seabird (M77-3 & M77-4: SBE-5; M90-M93: SBE  
209 43) oxygen sensor (Sea-Bird Electronics, Bellevue, WA, USA) mounted on the CTD rosette or from  
210 100 mL discrete samples taken from the Niskin bottles and analyzed using the Winkler titration  
211 method (Grasshoff et al., 1999). The oxygen sensor was calibrated against the Winkler  
212 measurements.

213 Recent studies using highly sensitive STOX (Switchable Trace amount Oxygen) sensors for oxygen  
214 measurements indicate that measurements with conventional oxygen sensors that are calibrated  
215 against Winkler measurements may be biased towards higher concentrations at near-zero oxygen  
216 conditions. Thamdrup et al. (2012) therefore argued that anoxic conditions are prevalent in the core  
217 of the Peruvian OMZ where oxygen concentrations of several  $\mu M$  have been found using the  
218 conventional Winkler-calibrated measurements. As STOX sensor measurements were not available  
219 for all measurement campaigns presented here, the minimum oxygen measurements reported here  
220 from the core of the OMZ (3-5  $\mu M$ ) should be considered as an overestimation.

221 The Apparent Oxygen Utilization (AOU) was calculated from the oxygen concentrations  $[O_2]_w$  using  
222 the CSIRO SeaWater library, version 3.2  
223 ([http://www.cmar.csiro.au/datacentre/ext\\_docs/seawater.htm](http://www.cmar.csiro.au/datacentre/ext_docs/seawater.htm)) to calculate oxygen saturation  
224  $[O_2]_{eq}$ :

$$225 \quad AOU = [O_2]_w - [O_2]_{eq} \quad (2)$$

226 Nutrient samples ( $[NO_3^-]$ ,  $[NO_2^-]$ ,  $[PO_4^{3-}]$ ,  $[NH_4^+]$ ) from the CTD rosette were analyzed onboard  
227 following the nutrient analysis methods according to Hansen et al. (1999). Samples taken from the  
228 pump-CTD during M77-3 were stored at -20°C and shipped to Germany for later analysis.  $N'$  was  
229 calculated as a measure for the nitrogen deficit from the nitrate ( $[NO_3^-]$ ), nitrite ( $[NO_2^-]$ ) and  
230 phosphate ( $[PO_4^{3-}]$ ) concentrations as follows (Altabet et al., 2012):

$$231 \quad N' = ([NO_3^-] + [NO_2^-]) - 16[PO_4^{3-}] \quad (3)$$

232 To distinguish between coastal and open ocean stations we calculated the distance of each station  
233 from the continental slope (2000 m isobath) and used the first baroclinic Rossby radius of  
234 deformation as described by Chelton et al. (1998) as threshold distance for stations that were  
235 influenced by coastal upwelling.

236

## 237     **3       Results**

### 238     **3.1      Spatial distribution of oxygen, nutrients and N<sub>2</sub>O**

239     The distribution of oxygen, nitrite and N<sub>2</sub>O along an offshore section between 16°S and 2°N at 86° W  
240     from the M77-4 cruise in 2009 and the M90 cruise in 2012 is shown in Figure 2; a coastal cross-shelf  
241     section along 12°S with the distribution of oxygen, nutrients, N' and N<sub>2</sub>O is shown in Figure 3 and  
242     selected depth profiles of oxygen, N<sub>2</sub>O and potential density ( $\sigma_\theta$ ) as well as nitrate, nitrite,  
243     ammonium and N' are shown in Figure 4.

244     Along 86° W, a similar distribution of oxygen, nitrite and N<sub>2</sub>O was observed during M77-4 and M90.  
245     Oxygen and N<sub>2</sub>O profiles concentrations were close to saturation in the mixed layer. The mixed layer  
246     depth increased from below 20 m in the northern part of the section to more than 100 m south of  
247     15 °S. Below the mixed layer, a sharp oxycline with a decrease to oxygen concentrations below  
248     10  $\mu$ M was observed south of 5°S, whereas in the northern part of the section, below the mixed layer  
249     oxygen concentrations only decreased to ~100  $\mu$ M in the upper 200 m and further dropped to  
250     concentrations ~10  $\mu$ M between 200 and 500 m. Minimum oxygen concentrations in the water  
251     column increased towards the north from below 5  $\mu$ M south of 5° S to ~10  $\mu$ M at the equator.

252     The nitrite distribution revealed a primary maximum at the base of the mixed layer with maximum  
253     nitrite concentrations below 1.5  $\mu$ M. This primary maximum is frequently observed in the ocean and  
254     is usually associated with nitrification (Codispoti and Christensen, 1985). South of 5° S, a secondary  
255     nitrite maximum was observed within the OMZ where oxygen concentrations fell below 5  $\mu$ M. Nitrite  
256     concentrations in the secondary maximum reached up to ~4  $\mu$ M.

257     Along the cross-shelf section at 12°S, the upper OMZ boundary significantly became shallower  
258     towards the coast as a signal of upwelling, with a well oxygenated mixed layer of ~50 m in the open  
259     ocean and a mixed layer depth of less than 5 m on the shelf. Oxygen was strongly undersaturated in  
260     the surface waters on the shelf as a result of upwelling of waters from the underlying OMZ (Fig. 4).  
261     Elevated phosphate concentrations in the surface waters at the coast also reflected the upwelling on

the shelf, whereas nitrate was depleted in the water column and the surface waters close to the coast, which was also reflected in very low  $N'$  values at the inshore stations (Fig. 3). A primary and secondary nitrite maximum at the base of the mixed layer and in the OMZ core was observed throughout the cross-shelf section, but both maxima were much more pronounced on the shelf than in the deep waters (Fig. 3).

The  $N_2O$  distribution along  $86^\circ W$  could be divided into two different regimes: north of  $5^\circ S$ , a broad  $N_2O$  maximum with concentrations of  $\sim 60$  nM coincided with the depth of the oxygen minimum, whereas in the southern part of the section, the  $N_2O$  profiles revealed a double-peak structure with a sharp  $N_2O$  maximum in the upper and lower oxycline and  $N_2O$  depletion in the OMZ core, also coinciding with the secondary nitrite maximum. This shape of  $N_2O$  profiles has been observed in OMZ regions before (e.g. Law and Owens, 1990; Cohen and Gordon, 1978). The transition from profiles with a broad  $N_2O$  peak to a double-peak structure coincided with the decrease in the minimum oxygen concentrations towards the South.  $N_2O$  depletion was observed in profiles where oxygen concentrations dropped below  $\sim 5$   $\mu M$  and nitrite accumulation was observed.

Compared to the offshore waters, the  $N_2O$  distribution on the shelf and in the adjacent waters showed a much larger variability.  $N_2O$  depletion was in fact observed at oxygen concentrations below 5  $\mu M$ , too. While several  $N_2O$  profiles revealed a shape similar to the offshore profiles, an overall characteristic shape could not be identified, however: profiles with a subsurface  $N_2O$  maximum in the oxycline were observed as well as profiles with multiple maxima or a surface  $N_2O$  maximum (Fig. 4).

While  $N_2O$  concentrations in the offshore waters did not exceed 80 nM,  $N_2O$  concentrations above 100 nM were frequently observed at the shelf. Several profiles showed an extreme  $N_2O$  accumulation with concentrations above 500  $\mu M$  (maximum  $\sim 850$  nM) (Fig. 4). The location and shape of the  $N_2O$  maxima in the different profiles was highly variable, which resulted in a very patchy distribution of  $N_2O$  in the water column (Fig. 3).

### 3.2 N<sub>2</sub>O in different water masses of the ETSP

The water mass distribution in our dataset agrees well with the data presented by Pietri et al. (2014) (Fig. 5). Due to the larger area covered by our measurements our data showed a broader scattering, but we could identify the same water masses in our data: below 500 m, both the coastal and the offshore profiles carry relatively fresh ( $S \sim 34.8$ ) and cool ( $T_{\text{pot}} \sim 5^\circ\text{C}$ ) Antarctic Intermediate Water (AAIW) (Pietri et al., 2014) that carried relatively high oxygen and  $\Delta\text{N}_2\text{O}$  values which corresponded to the secondary N<sub>2</sub>O maximum in the lower oxycline. Shallower subthermocline waters are covered by the Equatorial Subsurface Water (ESSW) ( $S \sim 34.8 - 35.2$ ,  $T_{\text{pot}} \sim 9-14^\circ\text{C}$ ) (Wyrki, 1967). This water mass carried very low oxygen down to concentrations, while  $\Delta\text{N}_2\text{O}$  values showed either a maximum or N<sub>2</sub>O depletion in this water mass, which reflects the strong sensitivity of net N<sub>2</sub>O consumption to variations in the oxygen concentration.

Waters with low salinities ( $\sim 34.7$ ), relatively high oxygen concentrations and potential temperatures between  $10^\circ\text{C}$  and  $15^\circ\text{C}$  can be traced back to Eastern South Pacific Intermediate Water (ESPIW) (Schneider et al., 2003).  $\Delta\text{N}_2\text{O}$  values within this water mass were between 20 and 30 nM. Pietri et al. (2014) identified narrow patches of ESPIW below the thermocline about  $\sim 100$  km offshore. We hardly found this water mass in the coastal data, but it is likely mixed with the ESSW and surface waters on the shelf, where it contributes to the formation of Cold Coastal Water (CCW) (Pietri et al., 2014). CCW with  $S \sim 35.1$  and  $T_{\text{pot}} \sim 15.5^\circ\text{C}$  was prevalent over the shelf and could only be identified in the coastal data as it is directly related to the coastal upwelling. Offshore surface data were associated with Subtropical Surface Water (STSW) with salinities above 35.0 and temperatures higher than  $17^\circ\text{C}$  (Pietri et al., 2013), while surface waters at the coast showed properties that resulted from the warming of the CCW and the mixing with STSW.

Very variable  $\Delta\text{N}_2\text{O}$  values were associated with the CCW and its related surface waters, and nearly all data points that showed extreme N<sub>2</sub>O accumulation fell within these waters. This indicates that

the extremely high  $\text{N}_2\text{O}$  concentrations were locally produced in the upwelling area, as none of the source water masses for the upwelling carried similarly high  $\Delta\text{N}_2\text{O}$  values.

### **3.3 $\Delta\text{N}_2\text{O}/\text{AOU}$ relationship**

A two-linear  $\Delta\text{N}_2\text{O}/\text{AOU}$  relationship has been identified in the upper oxycline for waters with oxygen concentrations higher than  $50\ \mu\text{M}$  and between  $50\ \mu\text{M}$  and  $5\ \mu\text{M}$  during the M77-4 cruise that took place in the offshore waters of the OMZ (Ryabenko et al., 2012). We found a very similar relationship for all offshore data with oxygen concentrations above  $50\ \mu\text{M}$  with no systematic difference between the data from the M77-4 (January/February 2009) cruise and the M90 (November 2012) cruise (Figures 2, 6a). This indicates a comparable setting of the open ocean OMZ waters during both cruises. We furthermore found no difference in the  $\Delta\text{N}_2\text{O}/\text{AOU}$  relationship between stations with a broad  $\text{N}_2\text{O}$  maximum and a double-peak structure. These results are similar to previously reported  $\Delta\text{N}_2\text{O}/\text{AOU}$  relationships from other oceanic OMZs (Upstill-Goddard et al., 1999; Cohen and Gordon, 1978; De Wilde and Helder, 1997).

In contrast to the open ocean waters, a correlation between  $\Delta\text{N}_2\text{O}$  and AOU was not observed for the coastal data (Fig. 6b). Numerous values with much higher  $\Delta\text{N}_2\text{O}/\text{AOU}$  ratios than in the offshore waters were observed. These data were highly scattered over the full range of oxygen concentrations. The  $\Delta\text{N}_2\text{O}$  values that showed the strongest deviation from the offshore  $\Delta\text{N}_2\text{O}/\text{AOU}$  ratio were associated with highly negative  $\text{N}'$  values as a signal for a large nitrogen deficit (Fig. 6b). This indicates that these waters with extreme  $\text{N}_2\text{O}$  accumulation had been subject to extensive N loss.

## 4 Discussion

To understand the differences between the offshore and the coastal N<sub>2</sub>O distribution in the Peruvian upwelling, the factors that influence N<sub>2</sub>O production or consumption during nitrification and denitrification need to be investigated.

In the oxycline waters of OMZs, peak N<sub>2</sub>O production from nitrification as well as denitrification has been determined under suboxic conditions, whereas N<sub>2</sub>O depletion was dominant in the OMZ core (Ji et al., 2015). Rate measurements however provided evidence that N<sub>2</sub>O production and consumption co-occur and that interplay between N<sub>2</sub>O production and consumption processes regulates net N<sub>2</sub>O accumulation or depletion in the water column (Babbin et al., 2015). In open ocean OMZs, however, N<sub>2</sub>O profiles reveal a remarkably stable shape which indicates that in these areas N<sub>2</sub>O production and consumption processes are well balanced (Babbin et al., 2015). Except for differences between the offshore N<sub>2</sub>O profiles with a broad N<sub>2</sub>O maximum north of 5 °S and a double-peak structure south of 5°S, the offshore N<sub>2</sub>O profiles observed in our study indeed showed a relatively invariant N<sub>2</sub>O distribution. The differences in the shape of the N<sub>2</sub>O profiles can be explained by changing oxygen concentrations in the OMZ core and a threshold oxygen concentration of 5 µM for net N<sub>2</sub>O consumption.

In areas where highly oxygen-deficient waters extended over the continental shelf, extreme accumulation of N<sub>2</sub>O has been found before in the Arabian Sea (Naqvi et al., 2010; Naqvi et al., 2006) and off Chile (Farías et al., 2015) and has been explained by rapid changes in the environmental conditions: Naqvi et al. (2000) explained the extreme N<sub>2</sub>O accumulation over the Indian shelf with the response of denitrifying enzymes to transient oxygen depletion. N<sub>2</sub>O thus accumulated when waters reached suboxic conditions. N<sub>2</sub>O accumulation coincided with the accumulation of nitrite and consumption of N<sub>2</sub>O started when these waters became sulfidic (Naqvi et al., 2010). Farías et al. (2015) measured N<sub>2</sub>O accumulation during the transition from oxic to anoxic conditions, too, but at variable oxygen concentrations whereas N<sub>2</sub>O depletion became dominant under suboxic conditions.



In contrast to the results from the Indian Ocean, they identified enhanced remineralization due to short-term variability in coastal upwelling as the main driver for N<sub>2</sub>O accumulation.

The large variability we observed in the N<sub>2</sub>O distribution at the Peruvian coast could also be explained by an imbalance between N<sub>2</sub>O production and consumption processes that may lead to its accumulation. This could have been induced by rapid changes of the oxygen concentrations in the coastal upwelling zone: enhanced mixing of oxygen-rich and oxygen deficient waters and exchange of upwelled waters with the atmosphere supply oxygen to the water column (Schafstall et al., 2010; Thomsen et al., 2016 ; Pietri et al., 2014) while strong remineralization leads to rapid oxygen consumption (Kalvelage et al., 2015). Kalvelage et al. (2011) furthermore showed that these high remineralization rates also induce strong N cycling in the subsurface layer. Turnover rates for different N species are therefore much faster on the shelf than in the open ocean OMZ (Hu et al., 2015), which is also reflected in the distribution of different functional gene abundances (Löscher et al., 2014). Hence, it is likely that N<sub>2</sub>O production and consumption rates are much higher at the coast than in the offshore waters, and that short periods of increased N<sub>2</sub>O production could lead to very high N<sub>2</sub>O accumulation.

Changes in the oxygen concentrations could influence N<sub>2</sub>O production from nitrification as well as from denitrification: enhanced production of N<sub>2</sub>O after transition from anoxic to oxic conditions is a known process occurring in soils (e.g. Morley et al., 2008 ) and may be explained by a different sensitivity of denitrifying enzymes to trace concentrations of oxygen (Tiedje, 1988). In a recent incubation study, Dalsgaard et al. (2014) found no indication of increased N<sub>2</sub>O production by denitrification due to changes in the oxygen concentration at nanomolar levels, however. Instead, autotrophic denitrification and N<sub>2</sub>O production have been shown to be stimulated by the addition of hydrogen sulfide (H<sub>2</sub>S) (Galan et al., 2014; Dalsgaard et al., 2014). We did not find direct evidence for a coupling between N<sub>2</sub>O production and the presence of H<sub>2</sub>S in our measurements, as high N<sub>2</sub>O accumulation was often found in proximity to H<sub>2</sub>S plumes but was also detected when H<sub>2</sub>S was absent in the water column. We cannot exclude that the high N<sub>2</sub>O production we frequently

observed at the shelf was stimulated by a coupling of denitrification with sulfur cycling, though: Canfield et al. (2010) found evidence for active sulfur cycling in the ETSP without H<sub>2</sub>S accumulation, and a coupling between H<sub>2</sub>S oxidation and denitrification has been shown before (Galan et al., 2014; Jensen et al., 2009). Indeed, active denitrification was found in proximity to H<sub>2</sub>S plumes in the water column during M77-3 (Kalvelage et al., 2013; Schunck et al., 2013).

In the ocean, increased N<sub>2</sub>O production was also associated with the onset of nitrification after re-ventilation of the water column in a seasonal study in the Baltic Sea, but with relatively low resulting N<sub>2</sub>O concentrations (Naqvi et al., 2010). Yu et al. (2010) found strongly increased N<sub>2</sub>O production by nitrifying bacteria that was stimulated by the availability of ammonium during recovery from anoxic conditions in a chemostat culture experiment. Their results point towards an increased N<sub>2</sub>O production via the ammonium-oxidation pathway, while N<sub>2</sub>O production by nitrifier-denitrification seemed not to be stimulated by the shift from anoxic to oxic conditions. We frequently measured high ammonium concentrations along the Peruvian shelf, indeed (Fig. 4), which could have stimulated N<sub>2</sub>O production from ammonium oxidation. A direct correlation between N<sub>2</sub>O and ammonium could not be identified, however.

From our concentration measurements alone we thus cannot distinguish if the observed high production of N<sub>2</sub>O is a result of denitrification or nitrification processes. Studies of the isotopic and isotopomeric N<sub>2</sub>O composition and N<sub>2</sub>O production and consumption rate measurements could reveal more detailed insights whether N<sub>2</sub>O is produced via the ammonium oxidation or the nitrite reduction pathway during its extreme accumulation.

In our study, we found strongly elevated N<sub>2</sub>O concentrations (>100 nM) over the full range of oxygen concentrations, coinciding with strong N depletion (Fig. 5), but without nitrite accumulation (Fig. 4). The high oxygen concentrations found in the majority of our samples with extreme N<sub>2</sub>O accumulation and N depletion excludes in-situ denitrification or anammox (see e.g. Babbin et al., 2014; Dalsgaard et al., 2014).

The extraordinarily high N<sub>2</sub>O concentrations as well as the low N' values thus have to be old signals of processes taking place under anoxic to suboxic conditions. There is no known consumption process for N<sub>2</sub>O in oxygenated waters (Bange, 2008), and the strong signals of N loss that are produced under anoxic conditions are unlikely to be rapidly compensated by N fixation upon oxygenation. Both signals thus are likely to have remained preserved when oxygen concentrations increased due to mixing with waters of higher oxygen concentration or due to direct contact with the atmosphere as a result of upwelling.

Our observations of high N<sub>2</sub>O concentrations in oxygenated waters furthermore indicate that this accumulation could have taken place during re-oxygenation rather than during decreasing oxygen concentrations. An increase in oxygen concentrations would lead to the preservation of the high N<sub>2</sub>O signals in the water column whereas further decreasing oxygen concentrations would only lead to a temporal N<sub>2</sub>O accumulation and would eventually stimulate N<sub>2</sub>O consumption.

#### **4 Summary and Conclusions**

We observed extreme N<sub>2</sub>O accumulations over the Peruvian shelf and in the adjacent waters with maximum concentrations similar to the observations by Naqvi et al. (2000) over the West Indian shelf and Fariás et al. (2015) off Chile, whereas N<sub>2</sub>O concentrations in the open ocean OMZ off Peru were comparably moderate. Similar to the findings by Naqvi et al. (2000), we found that N<sub>2</sub>O accumulation could be caused by enhanced N<sub>2</sub>O production by nitrification or denitrification under transient oxygen concentrations. We found strong evidence that these N<sub>2</sub>O accumulations are preserved when oxygen concentrations increased as a result of mixing and exchange with the overlying atmosphere in the upwelling zone. Waters with high N<sub>2</sub>O concentrations can thus be directly and frequently transported to the surface ocean. This makes this region one of the most important oceanic regions for N<sub>2</sub>O emissions to the atmosphere (Arévalo-Martínez et al., 2015). This direct link between unusually high N<sub>2</sub>O production and emissions over the Peruvian shelf makes it necessary to

understand the biogeochemical processes involved in N<sub>2</sub>O production and consumption to produce reliable predictions of oceanic emissions from this area. Current approaches to model the N<sub>2</sub>O distribution rely on parameterizations based on the linear  $\Delta\text{N}_2\text{O}/\text{AOU}$  relationship (Suntharalingam and Sarmiento, 2000; Nevison et al., 2003; Freing et al., 2012). These approaches could in fact reproduce the oxygen distribution in the open ocean OMZ off Peru reasonably well, but they fail to account for the extreme N<sub>2</sub>O accumulation and its high spatial and temporal variability over the shelf area. They thus significantly underestimate the emissions from the Peruvian upwelling and potentially other upwelling areas with similar conditions, too.

## Acknowledgements

We would like to thank the captains and crew of the R/V Meteor for their professional support and the chief scientists of M77-3 & M90-M93, Martin Frank, Lothar Stramma, Stefan Sommer and Gaute Lavik for the opportunity to collect samples during their cruises. We would also like to thank Annie Bourbonnais and Johanna Maltby for the collection of N<sub>2</sub>O samples during M92, and Gesa Eirund, Joel Craig, Georgina Flores, Jennifer Zur, Moritz Baumann, Tina Baustian and Dörte Nitschkowski for their help in analyzing the samples.

We would like to thank Frank Malien, Mirja Dunker, Violeta Leon, Peter Fritsche, Tina Baustian, Kerstin Nachtigall, Martina Lohmann, Gabriele Klockgether and Tim Kalvelage for the sampling and analysis of oxygen and nutrient samples during M77-3 & M77-4 and M90-M93. The work presented here was made possible by the DFG-supported projects SFB754 Phase I and II (<http://www.sfb754.de>) and the BMBF joint projects SOPRAN II and III (FKZ 03F0611A and FKZ 03F662A).

## 456 References

- 457 Altabet, M. A., Ryabenko, E., Stramma, L., Wallace, D. W. R., Frank, M., Grasse, P., and Lavik, G.: An  
458 eddy-stimulated hotspot for fixed nitrogen-loss from the Peru oxygen minimum zone,  
459 Biogeosciences, 9, 4897-4908, 10.5194/bg-9-4897-2012, 2012.
- 460 Arévalo-Martínez, D. L., Beyer, M., Krumbholz, M., Piller, I., Kock, A., Steinhoff, T., Kortzinger, A., and  
461 Bange, H. W.: A new method for continuous measurements of oceanic and atmospheric N<sub>2</sub>O, CO and  
462 CO<sub>2</sub>: performance of off-axis integrated cavity output spectroscopy (OA-ICOS) coupled to non-  
463 dispersive infrared detection (NDIR), Ocean Science, 9, 1071-1087, 10.5194/os-9-1071-2013, 2013.
- 464 Arévalo-Martínez, D. L., Kock, A., Löscher, C. R., Schmitz, R. A., and Bange, H. W.: Massive nitrous  
465 oxide emissions from the tropical South Pacific Ocean, Nature Geosci, 8, 530-533, 10.1038/ngeo2469  
466 [http://www.nature.com/ngeo/journal/vaop/ncurrent/abs/ngeo2469.html#supplementary-](http://www.nature.com/ngeo/journal/vaop/ncurrent/abs/ngeo2469.html#supplementary-information)  
467 information, 2015.
- 468 Arp, D. J., and Stein, L. Y.: Metabolism of inorganic N compounds by ammonia-oxidizing bacteria,  
469 Critical Reviews in Biochemistry and Molecular Biology, 38, 471-495, 10.1080/10409230390267446,  
470 2003.
- 471 Babbin, A. R., Keil, R. G., Devol, A. H., and Ward, B. B.: Organic Matter Stoichiometry, Flux, and  
472 Oxygen Control Nitrogen Loss in the Ocean, Science, 344, 406-408, 10.1126/science.1248364, 2014.
- 473 Babbin, A. R., Bianchi, D., Jayakumar, A., and Ward, B. B.: Rapid nitrous oxide cycling in the suboxic  
474 ocean, Science, 348, 1127-1129, 10.1126/science.aaa8380, 2015.
- 475 Bange, H. W., Andreae, M. O., Lal, S., Law, C. S., Naqvi, S. W. A., Patra, P. K., Rixen, T., and Upstill-  
476 Goddard, R. C.: Nitrous oxide emissions from the Arabian Sea: A synthesis, Atmospheric Chemistry  
477 and Physics, 1, 61-71, 2001.
- 478 Bange, H. W.: Gaseous nitrogen compounds (NO, N<sub>2</sub>O, N<sub>2</sub>, NH<sub>3</sub>) in the ocean, in: Nitrogen in the  
479 Marine Environment, 2 ed., edited by: Capone, D. G., Bronk, D. A., Mulholland, M. R., and Carpenter,  
480 E. J., Academic Press/Elsevier 51-94, 2008.
- 481 Canfield, D. E., Stewart, F. J., Thamdrup, B., De Brabandere, L., Dalsgaard, T., Delong, E. F., Revsbech,  
482 N. P., and Ulloa, O.: A Cryptic Sulfur Cycle in Oxygen-Minimum-Zone Waters off the Chilean Coast,  
483 Science, 330, 1375-1378, 10.1126/science.1196889, 2010.
- 484 Chaigneau, A., Dominguez, N., Eldin, G., Vasquez, L., Flores, R., Grados, C., and Echevin, V.: Near-  
485 coastal circulation in the Northern Humboldt Current System from shipboard ADCP data, Journal of  
486 Geophysical Research-Oceans, 118, 5251-5266, 10.1002/jgrc.20328, 2013.
- 487 Chang, B. X., Rich, J. R., Jayakumar, A., Naik, H., Pratihary, A. K., Keil, R. G., Ward, B. B., and Devol, A.  
488 H.: The effect of organic carbon on fixed nitrogen loss in the eastern tropical South Pacific and

489 Arabian Sea oxygen deficient zones, *Limnology and Oceanography*, 59, 1267-1274,  
 490 10.4319/lo.2014.59.4.1267, 2014.

491 Charpentier, J., Farias, L., and Pizarro, O.: Nitrous oxide fluxes in the central and eastern South  
 492 Pacific, *Global Biogeochemical Cycles*, 24, -, Artn Gb3011  
 493 Doi 10.1029/2008gb003388, 2010.

494 Chavez, F. P., and Messié, M.: A comparison of Eastern Boundary Upwelling Ecosystems, *Prog.*  
 495 *Oceanogr.*, 83, 80-96, 2009.

496 Chelton, D. B., DeSzoek, R. A., Schlax, M. G., El Naggar, K., and Siwertz, N.: Geographical variability  
 497 of the first baroclinic Rossby radius of deformation, *Journal of Physical Oceanography*, 28, 433-460,  
 498 10.1175/1520-0485(1998)028<0433:gvotfb>2.0.co;2, 1998.

499 Ciais, P., Sabine, C. L., Bala, G., Bopp, L., Brovkin, V., Canadell, J., Chhabra, A., DeFries, R., Galloway, J.  
 500 N., Heimann, M., Jones, C., Le Quéré, C., Myneni, R., Piao, S., and Thornton, P.: Carbon and other  
 501 Biogeochemical Cycles, in: *Climate Change 2013: The Physical Science Basis. Contribution of Working*  
 502 *Group I to the Fifth Assessment Report of the Intergovernmental Panel on Climate Change*, edited by:  
 503 Stocker, T. F., Qin, D., Plattner, G.-K., Tignor, M., Allen, S. K., Boschung, J., Nauels, A., Xia, Y., Bex, V.,  
 504 and Midgley, P. M., Cambridge University Press, Cambridge, UK, and New York, NY, USA, 465-570,  
 505 2013.

506 Codispoti, L. A., and Christensen, J. P.: Nitrification, denitrification and nitrous oxide cycling in the  
 507 eastern tropical South Pacific Ocean, *Marine Chemistry*, 16, 277-300, 1985.

508 Codispoti, L. A., Friederich, G. E., Packard, T. T., Glover, H. E., Kelly, P. J., Spinrad, R. W., Barber, R. T.,  
 509 Elkins, J. W., Ward, B. B., Lipschultz, F., and Lostaunau, N.: High nitrite levels off northern Peru: A  
 510 signal of instability in the marine denitrification rate, *Science*, 233, 1200-1202, 1986.

511 Cohen, Y., and Gordon, L. I.: Nitrous oxide in oxygen minimum of eastern tropical North Pacific -  
 512 evidence for its consumption during denitrification and possible mechanisms for its production,  
 513 *Deep-Sea Research*, 25, 509-524, 10.1016/0146-6291(78)90640-9, 1978.

514 Cornejo, M., and Farias, L.: Following the N<sub>2</sub>O consumption in the oxygen minimum zone of the  
 515 eastern South Pacific, *Biogeosciences*, 9, 3205-3212, 10.5194/bg-9-3205-2012, 2012.

516 Dalsgaard, T., Stewart, F. J., Thamdrup, B., De Brabandere, L., Revsbech, N. P., Ulloa, O., Canfield, D.  
 517 E., and DeLong, E. F.: Oxygen at Nanomolar Levels Reversibly Suppresses Process Rates and Gene  
 518 Expression in Anammox and Denitrification in the Oxygen Minimum Zone off Northern Chile, *Mbio*, 5,  
 519 UNSP e01966  
 520 10.1128/mBio.01966-14, 2014.

521 De Wilde, H. P. J., and Helder, W.: Nitrous oxide in the Somali Basin: the role of upwelling, *Deep Sea*  
 522 *Research Part II: Topical Studies in Oceanography*, 44, 1319-1340, [http://dx.doi.org/10.1016/S0967-](http://dx.doi.org/10.1016/S0967-0645(97)00011-8)  
 523 [0645\(97\)00011-8](http://dx.doi.org/10.1016/S0967-0645(97)00011-8), 1997.

524 Dewitte, B., Vazquez-Cuervo, J., Goubanova, K., Illig, S., Takahashi, K., Cambon, G., Purca, S., Correa,  
 525 D., Gutierrez, D., Sifeddine, A., and Ortlieb, L.: Change in El Nino flavours over 1958-2008:  
 526 Implications for the long-term trend of the upwelling off Peru, *Deep-Sea Res Pt II*, 77-80, 143-156,  
 527 10.1016/j.dsr2.2012.04.011, 2012.

528 Echevin, V., Aumont, O., Ledesma, J., and Flores, G.: The seasonal cycle of surface chlorophyll in the  
 529 Peruvian upwelling system: A modelling study, *Prog. Oceanogr.*, 79, 167-176,  
 530 <http://dx.doi.org/10.1016/j.pocean.2008.10.026>, 2008.

531 Farias, L., Paulmier, A., and Gallegos, M.: Nitrous oxide and N-nutrient cycling in the oxygen minimum  
 532 zone off northern Chile, *Deep-Sea Research Part I-Oceanographic Research Papers*, 54, 164-180,  
 533 10.1016/j.dsr.2006.11.003, 2007.

534 Farias, L., Castro-Gonzalez, M., Cornejo, M., Charpentier, J., Faundez, J., Boontanon, N., and Yoshida,  
 535 N.: Denitrification and nitrous oxide cycling within the upper oxycline of the eastern tropical South  
 536 Pacific oxygen minimum zone, *Limnology and Oceanography*, 54, 132-144, 2009.

537 Farías, L., Besoain, V., and García-Loyola, S.: Presence of nitrous oxide hotspots in the coastal  
 538 upwelling area off central Chile: an analysis of temporal variability based on ten years of a  
 539 biogeochemical time series, *Environmental Research Letters*, 10, 044017, 10.1088/1748-  
 540 9326/10/4/04, 2015.

541 Firestone, M. K., Firestone, R. B., and Tiedje, J. M.: Nitrous-oxide from soil denitrification - factors  
 542 controlling its biological production, *Science*, 208, 749-751, 10.1126/science.208.4445.749, 1980.

543 Forster, G., Upstill-Goddard, R. C., Gist, N., Robinson, C., Uher, G., and Woodward, E. M. S.: Nitrous  
 544 oxide and methane in the Atlantic Ocean between 50 degrees N and 52 degrees S: Latitudinal  
 545 distribution and sea-to-air flux, *Deep-Sea Res Pt II*, 56, 964-976, 10.1016/j.dsr2.2008.12.002, 2009.

546 Freing, A., Wallace, D. W. R., Tanhua, T., Walter, S., and Bange, H. W.: North Atlantic production of  
 547 nitrous oxide in the context of changing atmospheric levels, *Global Biogeochem. Cycles*, 23,  
 548 10.1029/2009gb003472, 2009.

549 Freing, A., Wallace, D. W. R., and Bange, H. W.: Global oceanic production of nitrous oxide,  
 550 *Philosophical Transactions of the Royal Society B-Biological Sciences*, 367, 1245-1255,  
 551 10.1098/rstb.2011.0360, 2012.

552 Fuenzalida, R., Schneider, W., Garcés-Vargas, J., Bravo, L., and Lange, C.: Vertical and horizontal  
 553 extension of the oxygen minimum zone in the eastern South Pacific Ocean, *Deep Sea Research Part*  
 554 *II: Topical Studies in Oceanography*, 56, 992-1003, 2009.

555 Galan, A., Faundez, J., Thamdrup, B., Francisco Santibanez, J., and Farias, L.: Temporal dynamics of  
 556 nitrogen loss in the coastal upwelling ecosystem off central Chile: Evidence of autotrophic  
 557 denitrification through sulfide oxidation, *Limnology and Oceanography*, 59, 1865-1878,  
 558 10.4319/lo.2014.59.6.1865, 2014.

559 Goreau, T. J., Kaplan, W. A., Wofsy, S. C., McElroy, M. B., Valois, F. W., and Watson, S. W.: Production  
 560 of  $\text{NO}_2^-$  and  $\text{N}_2\text{O}$  by nitrifying bacteria at reduced concentrations of oxygen, *Appl. Environ. Microbiol.*,  
 561 40, 526-532, 1980.

562 Graco, M., Purca, S., Dewitte, B., Morón, O., Ledesma, J., Flores, G., Castro, C., and Gutiérrez, D.: The  
 563 OMZ and nutrients features as a signature of interannual and low frequency variability off the  
 564 peruvian upwelling system, *Biogeosciences Discuss.*, 2016, 1-36, 10.5194/bg-2015-567, 2016.

565 Gutierrez, D., Enriquez, E., Purca, S., Quipuzcoa, L., Marquina, R., Flores, G., and Graco, M.:  
 566 Oxygenation episodes on the continental shelf of central Peru: Remote forcing and benthic  
 567 ecosystem response, *Prog. Oceanogr.*, 79, 177-189, 10.1016/j.pocean.2008.10.025, 2008.

568 Hamersley, M. R., Lavik, G., Woebken, D., Rattray, J. E., Lam, P., Hopmans, E. C., Sinninghe Damste, J.  
 569 S., Krueger, S., Graco, M., Gutierrez, D., and Kuypers, M. M. M.: Anaerobic ammonium oxidation in  
 570 the Peruvian oxygen minimum zone, *Limnology and Oceanography*, 52, 923-933, 2007.

571 Hansen, H. P., and Koroleff, F.: Determination of nutrients, in: *Methods of seawater analysis*, edited  
 572 by: Grasshoff, K., Kremling, K., and Ehrhardt, M., Wiley-VCH, Weinheim, 159-228, 1999.

573 Hu, H., Bourbonnais, A., Larkum, J., Bange, H. W., and Altabet, M. A.: Nitrogen cycling in shallow low  
 574 oxygen coastal waters off Peru from nitrite and nitrate nitrogen and oxygen isotopes, *Biogeosciences*  
 575 *Discuss.*, 12, 7257-7299, 10.5194/bgd-12-7257-2015, 2015.

576 IPCC: Climate Change 2013: The Physical Science Basis. Contribution of Working Group I to the Fifth  
 577 Assessment Report of the Intergovernmental Panel on Climate Change., Cambridge, UK and New  
 578 York, NY, 1535, 2013.

579 Jensen, M. M., Petersen, J., Dalsgaard, T., and Thamdrup, B.: Pathways, rates, and regulation of  $\text{N}_2$   
 580 production in the chemocline of an anoxic basin, Mariager Fjord, Denmark, *Marine Chemistry*, 113,  
 581 102-113, 10.1016/j.marchem.2009.01.002, 2009.

582 Ji, Q., Babbin, A. R., Jayakumar, A., Oleynik, S., and Ward, B. B.: Nitrous oxide production by  
 583 nitrification and denitrification in the Eastern Tropical South Pacific oxygen minimum zone,  
 584 *Geophysical Research Letters*, 42, 2015GL066853, 10.1002/2015gl066853, 2015.

585 Kalvelage, T., Jensen, M. M., Contreras, S., Revsbech, N. P., Lam, P., Guenter, M., LaRoche, J., Lavik,  
 586 G., and Kuypers, M. M. M.: Oxygen Sensitivity of Anammox and Coupled N-Cycle Processes in Oxygen  
 587 Minimum Zones, *Plos One*, 6, e29299  
 588 10.1371/journal.pone.0029299, 2011.

589 Kalvelage, T., Lavik, G., Lam, P., Contreras, S., Arteaga, L., Loescher, C. R., Oschlies, A., Paulmier, A.,  
 590 Stramma, L., and Kuypers, M. M. M.: Nitrogen cycling driven by organic matter export in the South  
 591 Pacific oxygen minimum zone, *Nature Geoscience*, 6, 228-234, 10.1038/ngeo1739, 2013.



592 Kalvelage, T., Lavik, G., Jensen, M. M., Revsbech, N. P., Loescher, C., Schunck, H., Desai, D. K., Hauss,  
593 H., Kiko, R., Holtappels, M., LaRoche, J., Schmitz, R. A., Graco, M. I., and Kuypers, M. M. M.: Aerobic  
594 Microbial Respiration In Oceanic Oxygen Minimum Zones, *Plos One*, 10, e0133526  
595 10.1371/journal.pone.0133526, 2015.

596 Karstensen, J., Stramma, L., and Visbeck, M.: Oxygen minimum zones in the eastern tropical Atlantic  
597 and Pacific oceans, *Prog. Oceanogr.*, 77, 331-350, 10.1016/j.pocean.2007.05.009, 2008.

598 Kock, A., and Bange, H. W.: Counting the ocean's greenhouse gas emissions, *Eos*, 96, 10-13,  
599 10.1029/2015EO023665, 2015.

600 Law, C. S., and Owens, N. J. P.: Significant flux of atmospheric nitrous oxide from the Northwest  
601 Indian Ocean, *Nature*, 346, 826-828, 10.1038/346826a0, 1990.

602 Löscher, C. R., Kock, A., Könneke, M., LaRoche, J., Bange, H. W., and Schmitz, R. A.: Production of  
603 oceanic nitrous oxide by ammonia-oxidizing archaea, *Biogeosciences*, 9, 2419-2429, 10.5194/bg-9-  
604 2419-2012, 2012.

605 Löscher, C. R., Grosskopf, T., Desai, F. D., Gill, D., Schunck, H., Croot, P. L., Schlosser, C., Neulinger, S.  
606 C., Pinnow, N., Lavik, G., Kuypers, M. M. M., LaRoche, J., and Schmitz, R. A.: Facets of diazotrophy in  
607 the oxygen minimum zone waters off Peru, *Isme Journal*, 8, 2180-2192, 10.1038/ismej.2014.71,  
608 2014.

609 Messie, M., Ledesma, J., Kolber, D. D., Michisaki, R. P., Foley, D. G., and Chavez, F. P.: Potential new  
610 production estimates in four eastern boundary upwelling ecosystems, *Prog. Oceanogr.*, 83, 151-158,  
611 10.1016/j.pocean.2009.07.018, 2009.

612 Montes, I., Colas, F., Capet, X., and Schneider, W.: On the pathways of the equatorial subsurface  
613 currents in the eastern equatorial Pacific and their contributions to the Peru-Chile Undercurrent,  
614 *Journal of Geophysical Research-Oceans*, 115, C09003  
615 10.1029/2009jc005710, 2010.

616 Morley, N., Baggs, E. M., Dorsch, P., and Bakken, L.: Production of NO, N(2)O and N(2) by extracted  
617 soil bacteria, regulation by NO(2)(-) and O(2) concentrations, *FEMS Microbiol. Ecol.*, 65, 102-112,  
618 10.1111/j.1574-6941.2008.00495.x, 2008.

619 Naqvi, S. W. A., Jayakumar, D. A., Narveka, P. V., Naik, H., Sarma, V. V. S. S., D'Souza, W., Joseph, S.,  
620 and George, M. D.: Increased marine production of N<sub>2</sub>O due to intensifying anoxia on the Indian  
621 continental shelf, *Nature*, 408, 346-349, 2000.

622 Naqvi, S. W. A., Naik, H., Pratihary, A., D'Souza, W., Narvekar, P. V., Jayakumar, D. A., Devol, A. H.,  
623 Yoshinari, T., and Saino, T.: Coastal versus open-ocean denitrification in the Arabian Sea,  
624 *Biogeosciences*, 3, 621-633, 2006.

625 Naqvi, S. W. A., Bange, H. W., Farias, L., Monteiro, P. M. S., Scranton, M. I., and Zhang, J.: Marine  
626 hypoxia/anoxia as a source of CH<sub>4</sub> and N<sub>2</sub>O, *Biogeosciences*, 7, 2159-2190, 10.5194/bg-7-2159-2010,  
627 2010.

628 Nevison, C., Butler, J. H., and Elkins, J. W.: Global distribution of N<sub>2</sub>O and the Delta N<sub>2</sub>O-AOU yield in  
629 the subsurface ocean, *Global Biogeochemical Cycles*, 17, 1119  
630 10.1029/2003gb002068, 2003.

631 Nevison, C. D., Lueker, T. J., and Weiss, R. F.: Quantifying the nitrous oxide source from coastal  
632 upwelling, *Global Biogeochem. Cycles*, 18, GB1018  
633 10.1029/2003GB002110, 2004.

634 Ni, B.-J., Peng, L., Law, Y., Guo, J., and Yuan, Z.: Modeling of Nitrous Oxide Production by Autotrophic  
635 Ammonia-Oxidizing Bacteria with Multiple Production Pathways, *Environmental Science &*  
636 *Technology*, 48, 3916-3924, 10.1021/es405592h, 2014.

637 Ostrom, N. E., Russ, M. E., Popp, B., Rust, T. M., and Karl, D. M.: Mechanisms of nitrous oxide  
638 production in the subtropical North Pacific based on determinations of the isotopic abundances of  
639 nitrous oxide and di-oxygen, *Chemosphere - Global Change Science*, 2, 281-290, 2000.

640 Paulmier, A., Ruiz-Pino, D., Garcon, V., and Farias, L.: Maintaining of the Eastern South Pacific Oxygen  
641 Minimum Zone (OMZ) off Chile, *Geophysical Research Letters*, 33, L20601  
642 10.1029/2006gl026801, 2006.

643 Pennington, J. T., Mahoney, K. L., Kuwahara, V. S., Kolber, D. D., Calienes, R., and Chavez, F. P.:  
644 Primary production in the eastern tropical Pacific: A review, *Prog. Oceanogr.*, 69, 285-317,  
645 10.1016/j.pocean.2006.03.012, 2006.

646 Pietri, A., Testor, P., Echevin, V., Chaigneau, A., Mortier, L., Eldin, G., and Grados, C.: Finescale  
647 Vertical Structure of the Upwelling System off Southern Peru as Observed from Glider Data, *Journal*  
648 *of Physical Oceanography*, 43, 631-646, 10.1175/jpo-d-12-035.1, 2013.

649 Pietri, A., Echevin, V., Testor, P., Chaigneau, A., Mortier, L., Grados, C., and Albert, A.: Impact of a  
650 coastal-trapped wave on the near-coastal circulation of the Peru upwelling system from glider data,  
651 *Journal of Geophysical Research-Oceans*, 119, 2109-2120, 10.1002/2013jc009270, 2014.

652 Ryabenko, E., Kock, A., Bange, H. W., Altabet, M. A., and Wallace, D. W. R.: Contrasting  
653 biogeochemistry of nitrogen in the Atlantic and Pacific Oxygen Minimum Zones, *Biogeosciences*, 9,  
654 203-215, 10.5194/bg-9-203-2012, 2012.

655 Santoro, A. E., Buchwald, C., McIlvin, M. R., and Casciotti, K. L.: Isotopic Signature of N(2)O Produced  
656 by Marine Ammonia-Oxidizing Archaea, *Science*, 333, 1282-1285, 10.1126/science.1208239, 2011.

657 Schneider, W., Fuenzalida, R., Rodriguez-Rubio, E., Garces-Vargas, J., and Bravo, L.: Characteristics  
658 and formation of eastern South Pacific intermediate water, *Geophysical Research Letters*, 30, 1581  
659 10.1029/2003gl017086, 2003.

660 Schunck, H., Lavik, G., Desai, D. K., Grosskopf, T., Kalvelage, T., Loescher, C. R., Paulmier, A.,  
661 Contreras, S., Siegel, H., Holtappels, M., Rosenstiel, P., Schilhabel, M. B., Graco, M., Schmitz, R. A.,  
662 Kuypers, M. M. M., and LaRoche, J.: Giant Hydrogen Sulfide Plume in the Oxygen Minimum Zone off  
663 Peru Supports Chemolithoautotrophy, *Plos One*, 8, e68661  
664 10.1371/journal.pone.0068661, 2013.

665 Stein, L. Y.: Surveying N<sub>2</sub>O-producing pathways in bacteria, in: *Methods in Enzymology: Research on*  
666 *Nitrification and Related Processes*, Vol 486, Part A, edited by: Klotz, M. G., *Methods in Enzymology*,  
667 131-152, 2011.

668 Stieglmeier, M., Mooshammer, M., Kitzler, B., Wanek, W., Zechmeister-Boltenstern, S., Richter, A.,  
669 and Schleper, C.: Aerobic nitrous oxide production through N-nitrosating hybrid formation in  
670 ammonia-oxidizing archaea, *Isme Journal*, 8, 1135-1146, 10.1038/ismej.2013.220, 2014.

671 Stramma, L., Johnson, G. C., Firing, E., and Schmidtko, S.: Eastern Pacific oxygen minimum zones:  
672 Supply paths and multidecadal changes, *Journal of Geophysical Research-Oceans*, 115, C09011  
673 10.1029/2009jc005976, 2010.

674 Suntharalingam, P., and Sarmiento, J. L.: Factors governing the oceanic nitrous oxide distribution:  
675 Simulations with an ocean general circulation model, *Global Biogeochemical Cycles*, 14, 429-454,  
676 10.1029/1999gb900032, 2000.

677 Thamdrup, B., Dalsgaard, T., Jensen, M. M., Ulloa, O., Farias, L., and Escribano, R.: Anaerobic  
678 ammonium oxidation in the oxygen-deficient waters off northern Chile, *Limnology and*  
679 *Oceanography*, 51, 2145-2156, 2006.

680 Thamdrup, B., Dalsgaard, T., and Revsbech, N. P.: Widespread functional anoxia in the oxygen  
681 minimum zone of the Eastern South Pacific, *Deep-Sea Research Part I-Oceanographic Research*  
682 *Papers*, 65, 36-45, 10.1016/j.dsr.2012.03.001, 2012.

683 Thomsen, S., Kanzow, T., Krahmann, G., Greatbatch, R. J., Dengler, M., and Lavik, G.: The formation of  
684 a subsurface anticyclonic eddy in the Peru-Chile Undercurrent and its impact on the near-coastal  
685 salinity, oxygen, and nutrient distributions, *Journal of Geophysical Research: Oceans*, n/a-n/a,  
686 10.1002/2015jc010878, 2016.

687 Tiedje, J. M.: Ecology of denitrification and dissimilatory nitrate reduction to ammonium, in: *Biology*  
688 *of anearobic microorganisms*, edited by: Zehnder, A. J. B., Wiley & Sons, New York, 179-244, 1988.

689 Upstill-Goddard, R. C., Barnes, J., and Owens, N. J. P.: Nitrous oxide and methane during the 1994 SW  
690 monsoon in the Arabian Sea/northwestern Indian Ocean, *Journal of Geophysical Research-Oceans*,  
691 104, 30067-30084, 10.1029/1999jc900232, 1999.

692 Walker, C. B., de la Torre, J. R., Klotz, M. G., Urakawa, H., Pinel, N., Arp, D. J., Brochier-Armanet, C.,  
693 Chain, P. S. G., Chan, P. P., Gollabgir, A., Hemp, J., Hugler, M., Karr, E. A., Konneke, M., Shin, M.,  
694 Lawton, T. J., Lowe, T., Martens-Habben, W., Sayavedra-Soto, L. A., Lang, D., Sievert, S. M.,  
695 Rosenzweig, A. C., Manning, G., and Stahl, D. A.: *Nitrosopumilus maritimus* genome reveals unique  
696 mechanisms for nitrification and autotrophy in globally distributed marine crenarchaea, *Proceedings*  
697 *of the National Academy of Sciences of the United States of America*, 107, 8818-8823,  
698 10.1073/pnas.0913533107, 2010.

699 Walter, S., Bange, H. W., Breitenbach, U., and Wallace, D. W. R.: Nitrous oxide in the North Atlantic  
700 Ocean, *Biogeosciences*, 3, 607-619, 10.5194/bg-3-607-2006, 2006.

701 Weiss, R. F., and Price, B. A.: Nitrous oxide solubility in water and seawater, *Mar. Chem.*, 8, 347-359,  
702 1980.

703 WMO: Scientific Assessment of Ozone Depletion: 2010, Global Ozone Research and Monitoring  
704 Project, Geneva, Switzerland, 2011.

705 Wyrski, K.: CIRCULATION AND WATER MASSES IN EASTERN EQUATORIAL PACIFIC OCEAN,  
706 *International Journal of Oceanology and Limnology*, 1, 117-&, 1967.

707 Yu, R., Kampschreur, M. J., Loosdrecht, M. C. M. v., and Chandran, K.: Mechanisms and Specific  
708 Directionality of Autotrophic Nitrous Oxide and Nitric Oxide Generation during Transient Anoxia,  
709 *Environmental Science & Technology*, 44, 1313-1319, 10.1021/es902794a, 2010.

710 Zamora, L. M., Oschlies, A., Bange, H. W., Huebert, K. B., Craig, J. D., Kock, A., and Loscher, C. R.:  
711 Nitrous oxide dynamics in low oxygen regions of the Pacific: insights from the MEMENTO database,  
712 *Biogeosciences*, 9, 5007-5022, 10.5194/bg-9-5007-2012, 2012.

713  
714

715

716

717 Figures:

718 Figure 1: Station maps of the sampled N<sub>2</sub>O stations from cruises A) M77-3, December 2008 – January  
719 2009 (●) and M77-4, January – February 2009 (○), B) M90, November 2012 (●) and M91,  
720 December 2012 (○), C) M92, January 2013 (●) and M93, February – March 2013 (○). Section  
721 annotations in A) and B) correspond to the vertical sections shown in Fig. 2 and 3.

722 Figure 2: Spatial distributions of oxygen (A, B), nitrite (C, D) and N<sub>2</sub>O (E, F) along 86°W during M77-4  
723 (2009, A, C, E) and M90 (2012, B, D, F). Small dots indicate location and depth of the discrete  
724 samples. Data gridding: ODV/DIVA.

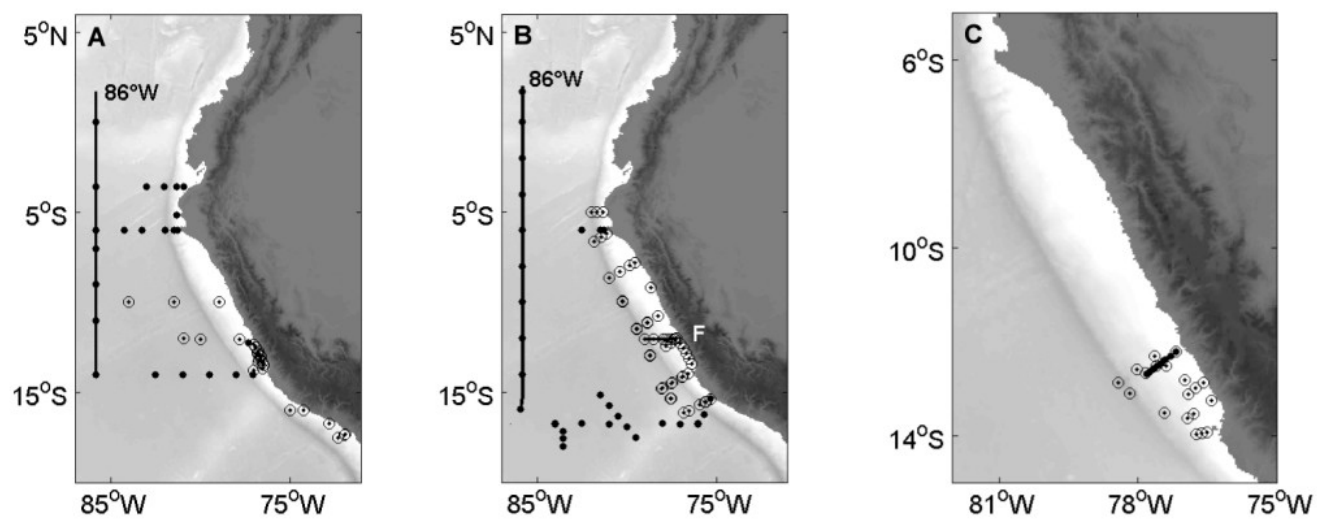
725 Figure 3: Cross-shelf distribution of A) Oxygen, B) Phosphate, C) Nitrate, D) N', e) Nitrite and f) N<sub>2</sub>O  
726 during M91 (Section F).

727 Figure 4: Selected depth profiles of oxygen (black dots, dotted line), potential density ( $\sigma_\theta$ , grey line)  
728 and N<sub>2</sub>O (red line, open circles) (left panel) and nitrate (grey line), nitrite (black circles, dotted  
729 line), ammonium (blue diamonds, straight line) and N' (red line, small dots) (right panel) from  
730 selected open ocean and shelf stations during M90-93. Depth profiles of oxygen and  $\sigma_\theta$  were  
731 taken from the CTD sensors, whereas the other parameters were taken from discrete samples.  
732 The locations of the respective stations are shown in the map. Red signals denote stations  
733 classified as “coastal” stations whereas blue signals denote “offshore” stations. Please note the  
734 changes in the scales for N<sub>2</sub>O,  $\sigma_\theta$ , nitrite and ammonium.

735 Figure 5: Temperature-Salinity diagrams with  $\Delta$ N<sub>2</sub>O color coded for a) the offshore stations and b)  
736 the onshore stations. Gray symbols denote the T-S properties of a) the onshore and b) the  
737 offshore data. The approximate location of the different water masses annotated in the figure is  
738 given by black dots or lines. Different symbols denote different cruises: □ M77-3; ◇ M77-4; ○  
739 M92; ▷ M90; ◁ M91; ✱ M93.

Figure 6:  $\Delta N_2O$ /AOU relationship from a) offshore stations and b) coastal stations. Samples from the upper OMZ and oxycline (sample depth < 350 m) are color coded with  $N'$ , whereas samples from below 350 m are shown in gray. Different symbols for different cruises are denoted the same as in Figure 5. The black line denotes the  $\Delta N_2O$ /AOU relationship from the offshore data for samples with  $O_2 > 50 \mu M$  and depth < 350 m ( $y = 0.13x + 3.73$ ;  $r^2 = 0.83$ ). Please note the change in the scaling for  $\Delta N_2O$  values of 0 - 100 nM and 100 - 1000 nM (dotted line).

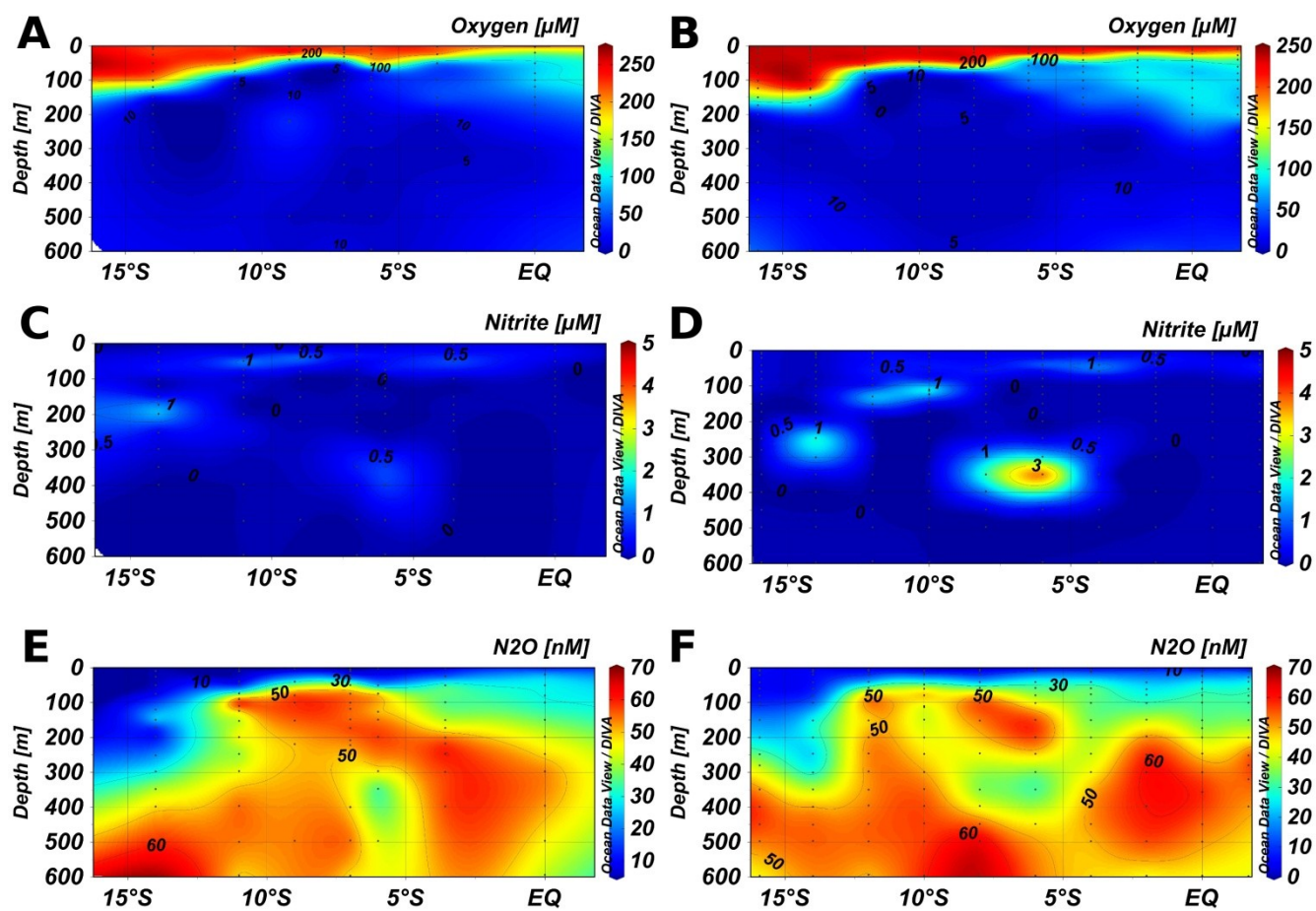
747 Figure 1:



748

749

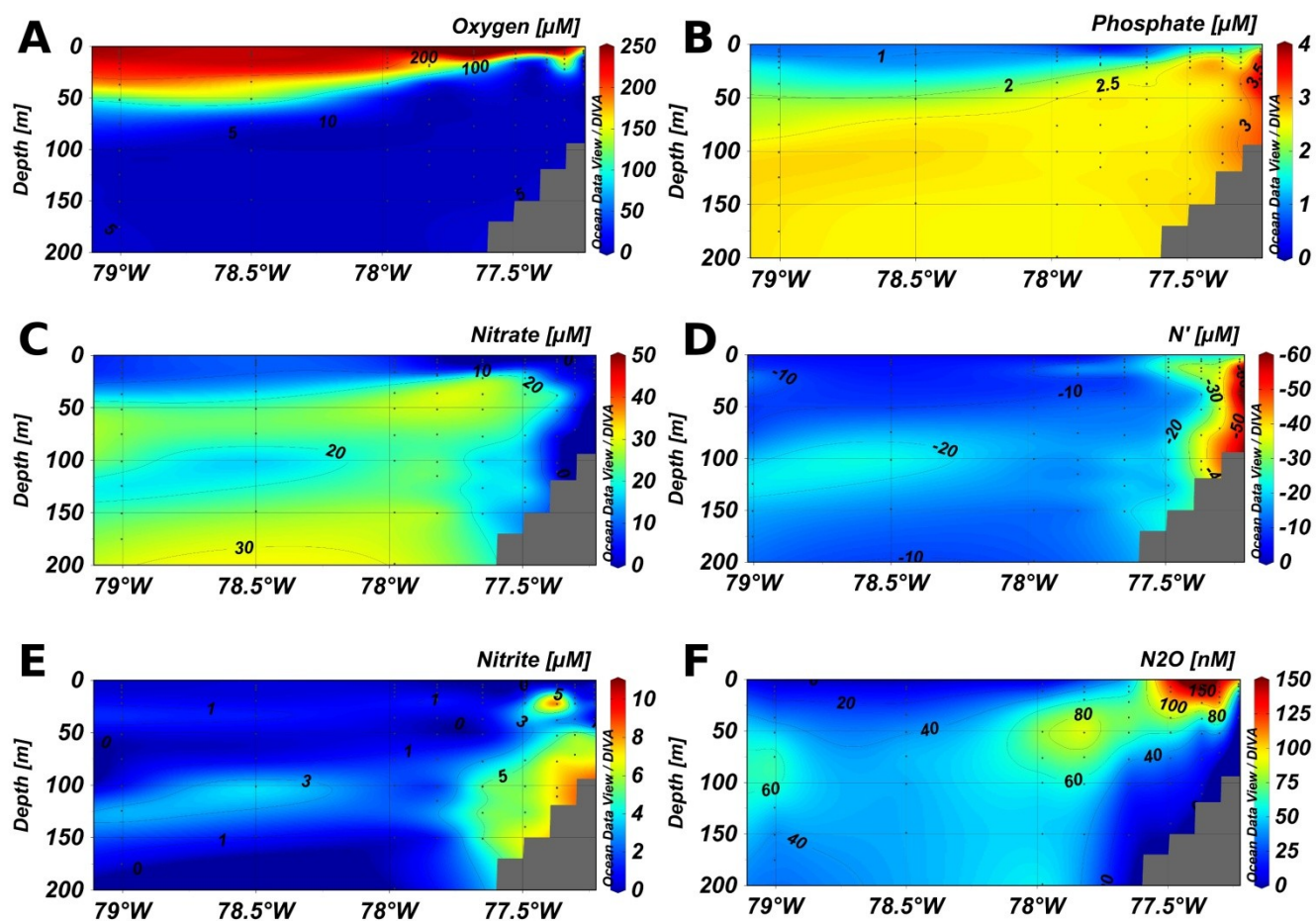
750 Figure 2:



751  
752



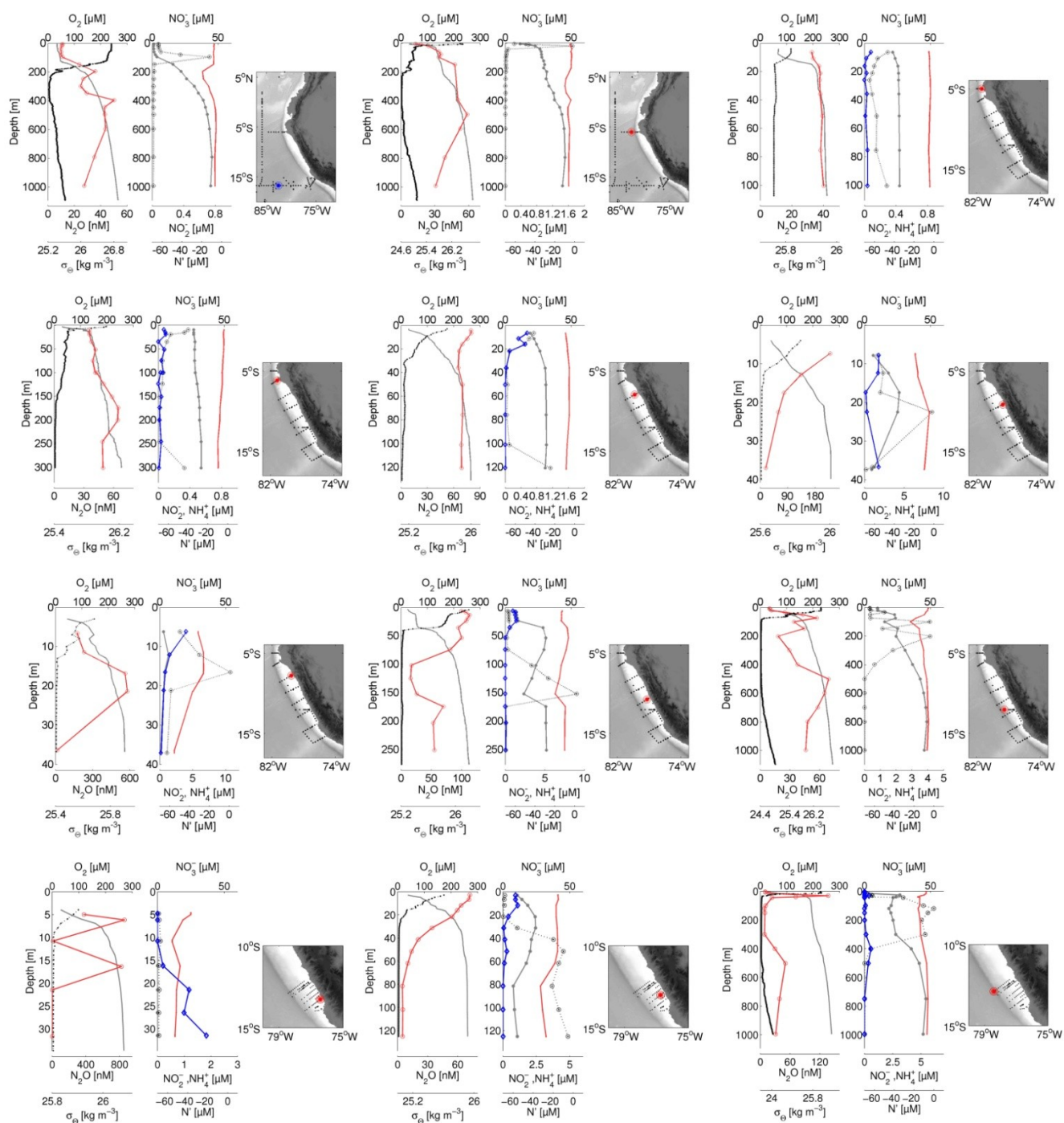
753 Figure 3:



754

755

756 Figure 4:



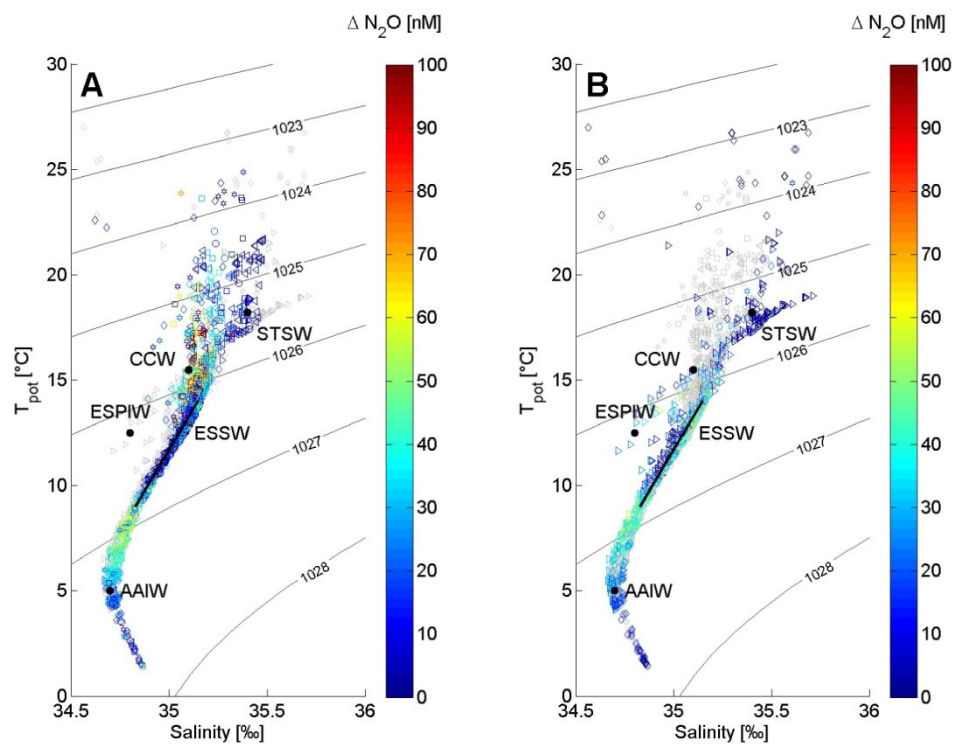
757

758

759

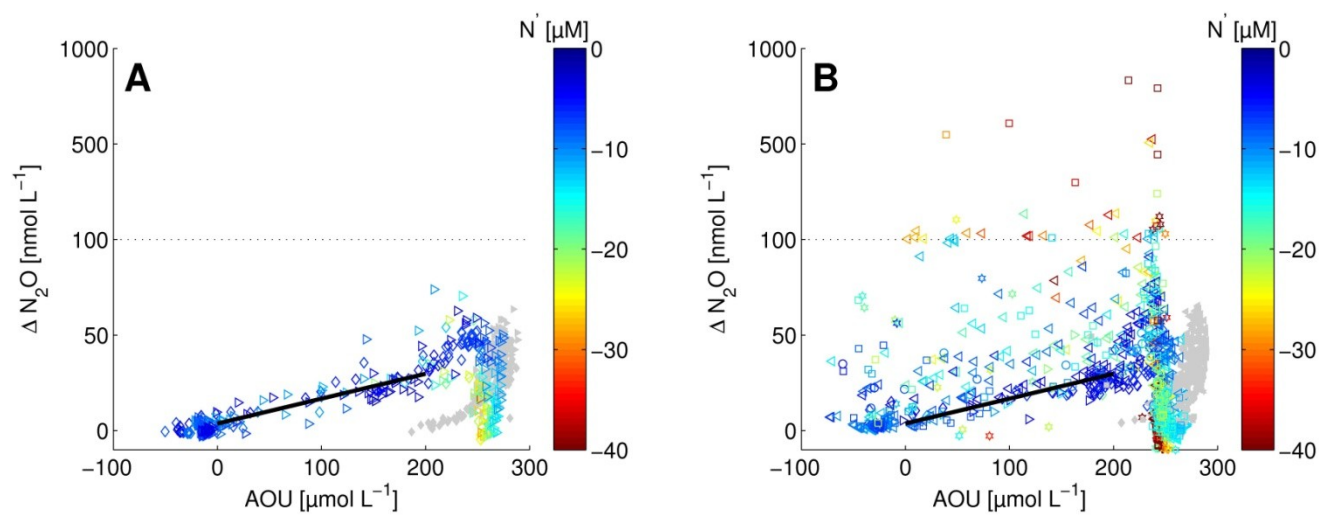
760 Figure 5:

761



762

763      Figure 6:



764

765

766

767